EPJ Web of Conferences **52**, 01010 (2013)
DOI: 10.1051/epjconf/20135201010

New results from the NA49 experiment on hadron production in p+p and p+C interactions and survey of backward hadrons in p+C collisions

M. Makariev[1,a] for the NA49 collaboration

[1] *Institute for Nuclear Research and Nuclear Energy, Bulgarian Academy of Sciences, Sofia, Bulgaria*

Abstract. Recent results on proton, anti-proton, neutron and charged kaon production in proton-proton and proton, anti-proton, neutron, deuteron and triton production in proton-carbon collisions at 158 GeV/c beam momentum are presented. Data samples of 4.8 million and 385 734 inelastic events in p+p and p+C, respectively, are obtained with the NA49 detector at the CERN SPS accelerator. The charged particles are identified by energy loss measurement in a system of four TPC chambers, while the neutrons are detected in a forward hadronic calorimeter. The data cover a major fraction of the phase space, ranging from 0 to 1.9 GeV in p_T and in Feynman x variable from -0.8 to 0.95 for protons, from -0.2 to 0.3 for anti-protons, from 0.1 to 0.95 for neutrons and from 0 to 0.5 for kaons. The comparison of the results on proton and neutron production in p+p interactions and deep inelastic e+p collisions at HERA reveals an independence of target fragmentation on the projectile type. Using the charged kaon data in p+p collisions as a reference, a new evaluation of the energy dependence of kaon production, including neutral kaons, is conducted over a range from 3 GeV to p+$\overline{\text{p}}$ collider energies. A survey of backward production of protons and pions in p+C collisions in the range of lab angles from 10 to 180 degrees, from 0.2 to 1.2 GeV/c in lab momentum and from 1 to 400 GeV/c in projectile momentum has been performed.

1 Introduction

In the absence of quantitative prediction in the non-perturbative sector of QCD, the study of soft hadronic physics has to rely on self-consistent high statistics data sets, including a variety of projectile and target combinations. In addition full phase space coverage with complete particle identification and small systematic uncertainty is required.

The NA49 experiment aims at providing such data sets ranging from elementary hadron-proton collisions to hadron-nucleus and nucleus-nucleus interactions, obtained using the same detector layout combining wide acceptance, systematic uncertainty of less than 5% and complete particle identification via measurement of specific energy loss. It is therefore well suited for the comparison of the different processes and to a detailed scrutiny of the evolution from elementary to nuclear hadronic phenomena and thus providing a basis for a model independent study to the underlying production mechanisms.

In the framework of this extensive experimental program the NA49 experiment has already published papers concerning pion [1], baryon [2] and kaon [3] production in p+p collisions, and pion [4, 5] production in p+C collisions. Two new articles have been submitted for publication regarding baryon and light ion production [6] and a survey of backward production of protons and pions from 1 to 400 GeV/c beam momentum [7] in p+C interactions.

[a] e-mail: makariev@inrne.bas.bg

In this paper the recent results from [2, 3, 6, 7] will be discussed.

2 Data sets

The data sets obtained by the NA49 experiment are summarized in Fig. 1.

Table 1. The data sets obtained by the NA49 experiment.

hadron-proton	hadron-nucleus	nucleus-nucleus
p + p	d + p	Pb + Pb
n + p	p + C	
π^+ + p	p + Pb	
π^- + p	π^+ + Pb	
	π^- + Pb	

3 Variables and cross section definition

The NA49 experiment establishes the invariant double differential cross sections

$$f(x_F, p_T) = E(x_F, p_T) \cdot \frac{d^3\sigma}{dp^3}(x_F, p_T). \quad (1)$$

Here p_T is the transverse momentum and x_F is the reduced longitudinal momentum:

$$x_F = \frac{p_L}{\sqrt{s}/2} \quad (2)$$

where p_L denotes the longitudinal momentum component in the center-of-mass system (cms). For the neutrons, due to the lack of transversal granularity of the NA49 calorimeter, only p_T-integrated density distributions:

$$dn/dx_F = \pi/\sigma_{\text{inel}} \cdot \sqrt{s}/2 \cdot \int f/E \cdot dp_T^2 \qquad (3)$$

will be presented, with σ_{inel} being total inelastic cross section.

4 Results from p+p interactions

4.1 Baryons

It total 333 cross sections for protons and 143 for anti-protons have been derived, with systematic errors of 2.5% for protons and 3.3% for anti-protons, respectively, see [2]. The data cover the range in x_F from -0.05 to 0.95 (-0.05 to 0.4) and in p_T from 0 to 1.9 GeV/c (0 to 1.5 GeV/c) for protons (anti-protons). An example of x_F distributions of protons at fixed p_T is shown in Fig. 1.

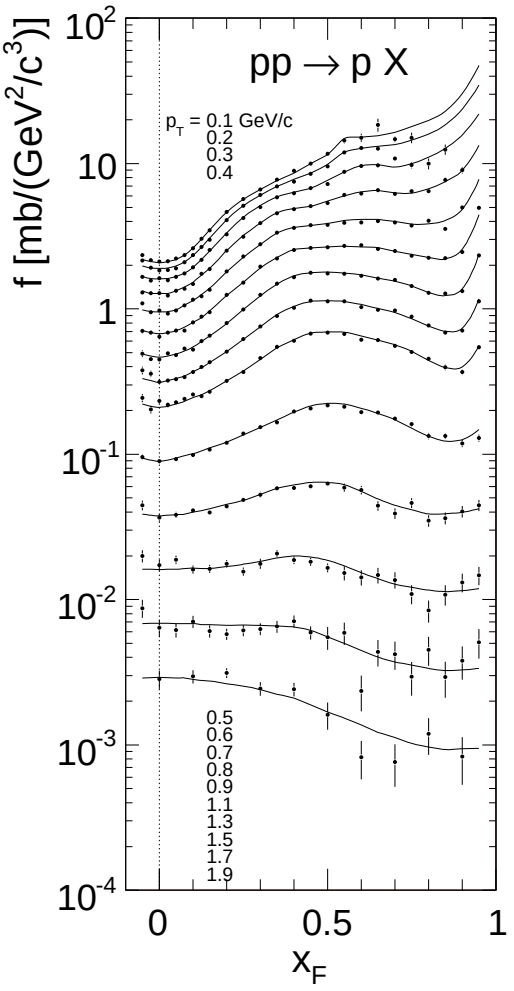

Figure 1. Double differential invariant cross section $f(x_F, p_T)$ [mb/(GeV^2/c^3)] as a function of x_F at fixed p_T for protons produced in p+p collisions at 158 GeV/c beam momentum. The lines show the result of the interpolation of the data.

As the NA49 detector acceptance is limited at low p_T and large x_F the results from other measurements have been used to supplement the NA49 data, for a detailed discussion see [2]. The dense coverage allows for precise determination of integrated quantities which are also available in [2].

The p_T integrated density distribution dn/dx_F for neutrons is presented in Fig. 2 as a function of x_F. The K_L^0 and $\overline{n}$ distributions, which have been subtracted from the total measured yields, are also shown in the figure.

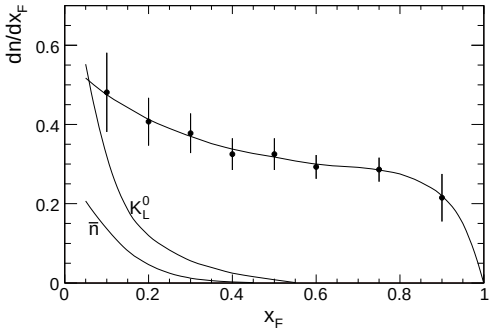

Figure 2. p_T integrated density distribution dn/dx_F as a function of x_F of neutrons produced in p+p interactions at 158 GeV/c. The subtracted K_L^0 and anti-neutron distributions are also shown.

4.2 Comparison to e+p collisions at HERA

Data from the ZEUS collaboration at HERA concerning proton [8] and neutron [9] production in the target hemisphere provide results at mean energies of about 130 GeV in the photon-proton cms. These data allow for a rather detailed comparison of the e+p and p+p interactions.

The ZEUS data cover a range from 0.1–0.7 GeV/c in p_T and from 0.6 to 0.99 in x_F for protons [8], and from 0.05 to 0.6 GeV/c in p_T and from 0.26 to 0.97 in x_F for neutrons [9]. The comparison of the shape of the p_T distributions with the proton results from NA49 (full lines), normalized to the ZEUS data, is shown in Figs. 3 and 4.

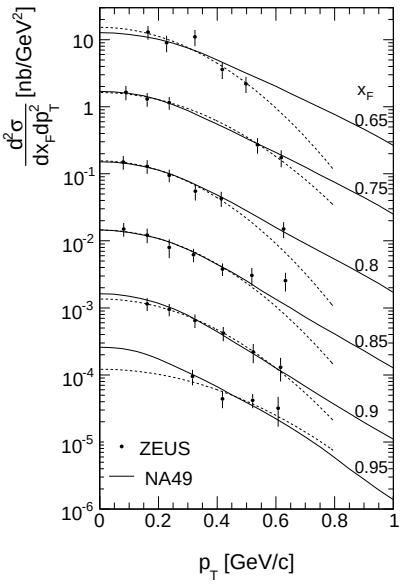

Figure 3. Comparison of the proton p_T distributions at several x_F values of the NA49 results (full lines) with measurements from [8]. The data were successively divided by 10 for different x_F values for better separation. The dashed lines represent the parametrization used in [8].

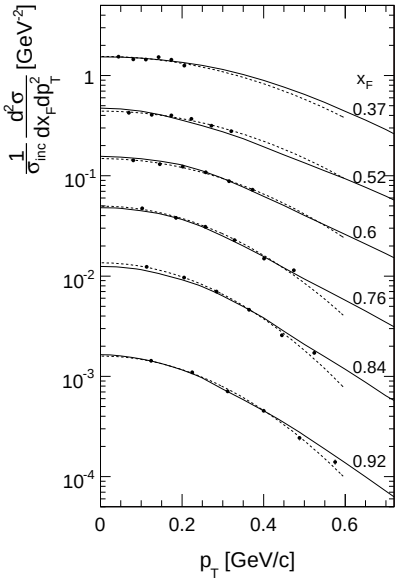

Figure 4. Comparison of the p_T distributions at different x_F values of protons from NA49 (full lines) with neutrons from [9]. The data were successively divided by 3 for different x_F values for better separation. The dashed lines represent the parametrization used in [9].

This comparison reveals that the shape of the p_T distributions is similar between the protons and neutrons as well as between the different interactions. Also the absolute proton and neutron densities have been shown to be equal in e+p and p+p collisions [2], corresponding to hadronic factorization.

4.3 Kaons

The results on kaon production consist of 158 data points for each K^+ and K^-. They cover a range from 0 to 1.7 GeV/c in p_T and from 0 to 0.4 (0.5) in x_F for K^+ (K^-) with a systematic uncertainty of 2.2% at $x_F < 0.25$ and up to 10% for K^+ and 6% for K^- at larger x_F. As in the case of baryons the integrated quantities have been established with high precision.

As the interaction energy of $\sqrt{s}$ = 17.2 GeV is located at a strategical point between threshold-dominated and scaling phenomena at lower and higher energies, respectively, a new and complete study of the s-dependence of kaon production including K^0_S has been attempted using the new NA49 data as a reference. This study covers the energy range $3 < \sqrt{s} < 1800$ GeV and aims at establishing an internally consistent picture of kaon production. The $\sqrt{s}$ dependence of the total kaon yields $\langle n_K \rangle$ is presented in Fig. 5.

This new evaluation should replace the data from [10] which show an unphysical behaviour of charged kaon yield [3]. These results also prove the validity of the relation $K^0_S = 0.5(K^+ + K^-)$ for $\sqrt{s} > 5$ GeV.

5 Results from p+C interactions

5.1 Baryons

The data from p+C collisions cover a phase space area ranging from 0 to 1.9 GeV/c in transverse momentum and from -0.80 to 0.95 for protons and from -0.2 to 0.3 for anti-protons in x_F [6]. This results in 491 and 121 cross

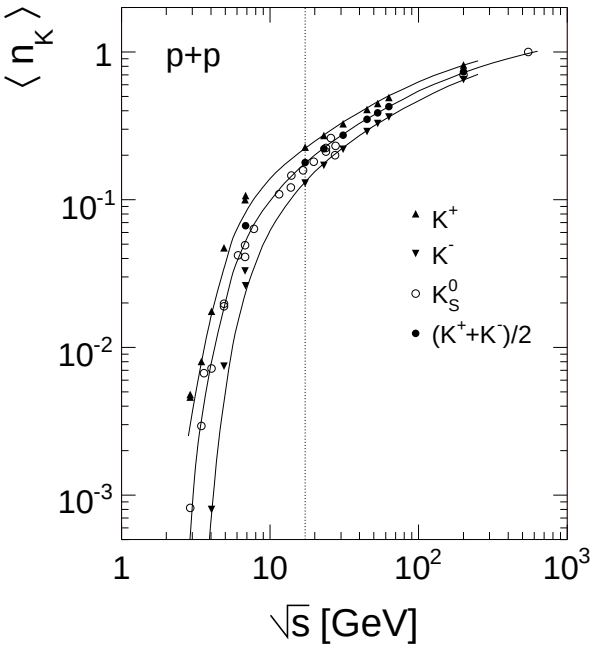

Figure 5. Total yields $\langle n_{K^+} \rangle$, $\langle n_{K^-} \rangle$ and $\langle n_{K^0_S} \rangle$ as a function of $\sqrt{s}$. The full line through the K^0_S is the result of an eyeball fit, the lines through the K^+ and K^- data are derived from [3]. The full circles in the K^0_S data correspond to $0.5(\langle n_{K^+} \rangle + \langle n_{K^-} \rangle)$ established at the corresponding $\sqrt{s}$ values.

section values for protons and anti-protons, respectively. Existing data [11], which are complementary to the NA49 measurements, in the far backward hemisphere are used to extend the coverage for protons into the region of intranuclear cascading, see [6]. The corresponding proton x_F distributions, which cover the phase space from x_F =-2 up to the kinematic limit at $x_F \sim +1$, are shown in Fig. 6. Both the NA49 data (full circles) and [11] (open circles) are plotted.

Several interesting features should be mentioned:

- The kinematic limit extends far below x_F = -1.
- There is no indication of diffractive peak at $x_F \sim$ -1.
- The maximum of the distributions in backward region is located at $x_F \sim$ -0.92 rather than x_F = -1.

The p_T integrated dn/dx_F distributions for protons and neutrons are presented in Fig. 7 in the projectile hemisphere together with the neutron results from p+p collisions (dotted lines). Protons and neutrons show within errors the same transfer towards the center when passing from p+p to p+C reaction. The densities are equal at $x_F \sim 0.3$. Densities from p+C are bigger at lower x_F, reaching increase of about 1.3 at $x_F = 0.1$, and smaller at larger x_F decreasing to 0.6 of the p+p densities at x_F towards +1. The latter value corresponds to the expected fraction of single projectile collisions in p+C interactions derived from the nuclear density distribution and from the inelastic cross sections [5].

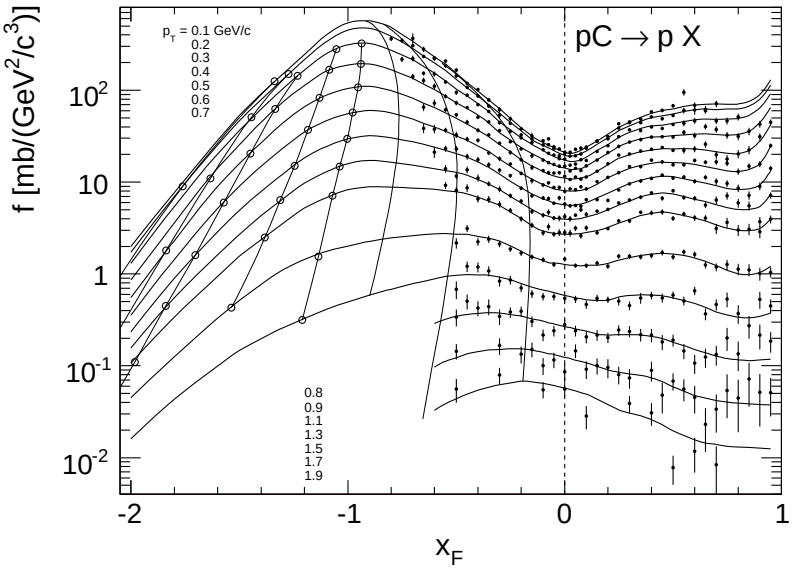

Figure 6. Invariant cross sections at fixed p_T as a function of x_F. Full circles: NA49 data, open circles: data from [11]. The thin lines show the cross section at fixed angles of 10^o, 30^o and 50^o.

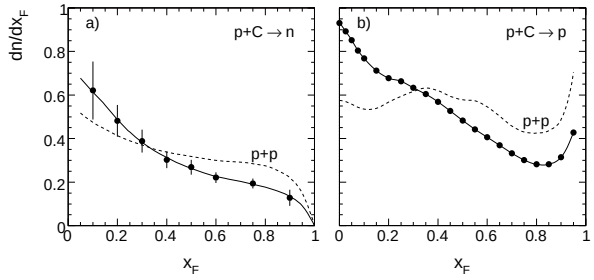

Figure 7. The p_T integrated neutron and proton density distribution dn/dx_F in p+C (full circles) and in p+p (dotted line) collisions.

5.2 Deuterons and tritons

Deuterons and tritons can be identified via specific energy loss measurement by the NA49 detector at lab momenta below 2 GeV/c for deuterons and 3 GeV for tritons. The density ratio of deuterons to protons R_d and tritons to protons R_t are shown in Fig. 5.2 as a function of x_F, where the transformation from lab to cms system is performed assuming the proton mass. In the figure are also presented the results from [12] (open symbols) which show good agreement as in the case of the proton data [11]. The ratio R_t is suppressed with respect to R_d by a factor of 0.1 to 0.2 depending on p_T but independent on x_F. These ratios are for the first time available at low p_T and in the approach to $x_F = 0$, where R_d decreases to values of about 1%.

5.3 Three component mechanism

The final state of p+A collisions consists of three basic components:

- The fragmentation of the projectile particle
- The fragmentation of the target nucleons
- The intra-nuclear cascading, generated by the interaction of the participating nucleons and secondary produced hadrons inside the nucleus.

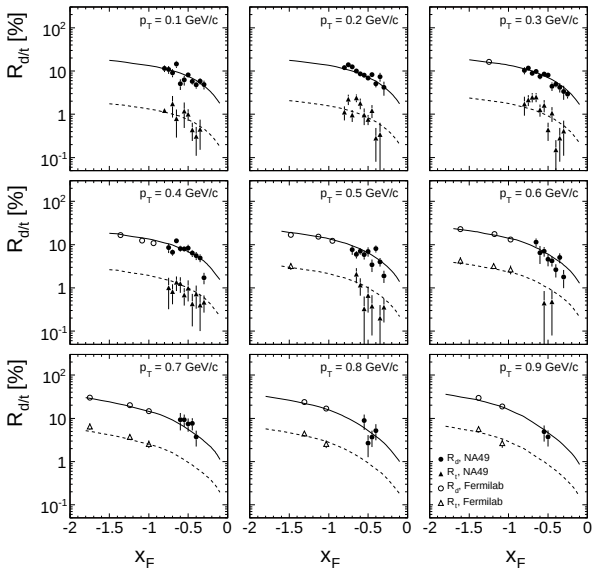

Figure 8. Deuteron and triton to proton density ratios R_d and R_t as a function of x_F for fixed values of p_T between 0.1 and 0.9 GeV/c. The full lines give the two-dimensional data interpolation established for R_d, the broken lines are the same multiplied by the suppression factors, assumed x_F independent, see [6].

These components have been separated and quantified for pion production [5, 7] and baryon production [6] in p+C collisions. An example of the net proton p_T integrated dn/dx_F distribution is shown in Fig. 9 where the total yield and the three components are indicated with different lines.

It has to be noted that this separation relies essentially on experimental input. There is only one assumption made concerning the target component and no other free parameters are used in the analysis. The target component is predicted from p+p collisions, assuming that the hadronization of the hit target nucleus is equivalent to the hadronization of the elementary nucleon-nucleon interactions, taking into account the isospin symmetry and multiplying by the mean number of collisions $\langle \nu \rangle$ that the projectile suf-

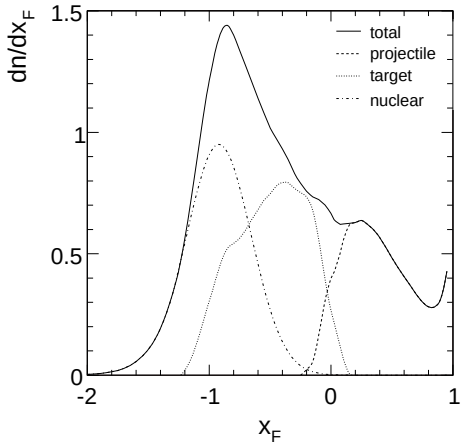

Figure 9. The nuclear, target and projectile components for protons in p+C collisions.

fers on its way through the target nucleus, see [6]. For the p+C interaction $\langle\nu\rangle$ is equal to 1.6, see [4]. The projectile and nuclear components follow, without additional assumptions, from the subtraction of the target fragmentation from the measured total yield.

6 Survey of backward production of protons and pions in p+C interactions

In Sect. 5.1, Fig. 6, it was shown that backward proton production is peaked at around x_F = -0.92 and not at x_F = -1. One mechanism for this baryon transfer can be pion production in intra-nuclear cascading [2]. To study this phenomenon a survey of backward production of protons and pions in p+C collisions has been performed [7]. This survey covers the region of $\Theta_{\rm lab}$ from 10 to 180 degrees, $p_{\rm lab}$ from 0.2 to 1.2 GeV/c and beam momentum $p_{\rm beam}$ from 1 to 400 GeV/c. About 3500 data points coming from 19 experiments have been localized [7]. As these experiments use in general different variables and binning, all results were transformed to invariant cross sections (1) and expressed in the three variables $\Theta_{\rm lab}$, $p_{\rm lab}$ and $1/\sqrt{s}$. A three dimensional interpolation in these three variables was performed which uses the physics constraints of smoothness, continuity and regularity at the phase space boundaries, for details see [7]. An example of π^- distributions as a function of $1/\sqrt{s}$ at fixed $p_{\rm lab}$ and $\Theta_{\rm lab}$ = 67 degrees together with the global data interpolation is presented in Fig. 10.

The data interpolation establishes a strong constraint for possible experimental deviations. In fact 4 of the 19 data sets have been shown to be inconsistent with all other results.

7 Conclusions

New inclusive data on kaon and baryon production in p+p interactions and baryon and light ion production in p+C collisions at 158 GeV/c beam momentum have been presented. These results are part of the systematic study of soft hadronic interactions by the NA49 experiment, combining wide phase space coverage and systematic errors below 5%.

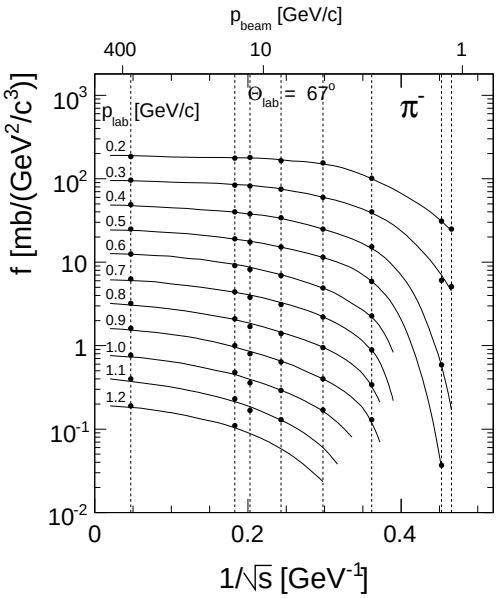

Figure 10. Invariant cross sections for π^- in p+C collisions as a function of $1/\sqrt{s}$ at fixed $p_{\rm lab}$ and $\Theta_{\rm lab}$ = 67 degrees. The solid lines represent the global data interpolation.

The comparison of the results on proton and neutron production in p+p interactions and deep inelastic e+p collisions at HERA reveals hadronic factorization in the target fragmentation region.

New evaluation of kaon yields in p+p collisions has been established in the range $3 < \sqrt{s} < 1800$ GeV where the relation $K^0_S = 0.5(K^+ + K^-)$ is shown to be valid for $\sqrt{s} > 5$ GeV.

A survey of backward production of protons and pions in the range of lab angles from 10 to 180 degrees, from 0.2 to 1.2 GeV/c in lab momentum and from 1 to 400 GeV/c in projectile momentum has been performed. Over 3500 data points from 19 experiments have been used in order to establish a consistent description of proton and pion production in the backward hemisphere.

Acknowledgements

This work was supported by the Bulgarian National Science Fund (Ph-09/05).

References

[1] C. Alt et al., Eur. Phys. J. **C45** (2006) 343
[2] T. Anticic et al., Eur. Phys. J. **C65** (2010) 9
[3] T. Anticic et al., Eur. Phys. J. **C68** (2010) 1
[4] C. Alt et al., Eur. Phys. J. **C49** (2007) 897
[5] G. Barr et al., Eur. Phys. J. **C49** (2007) 919
[6] B. Baatar et al., arXiv:1207.6520v1[hep-ex]
[7] O. Chvala et al., arXiv:1210.6775[nucl-ex]
[8] S. Chekanov et al., Nucl. Phys. **B658** (2003) 3
[9] S. Chekanov et al., Nucl. Phys. **B776** (2007) 1
[10] A. M. Rossi et al., Nucl. Phys. **B84** (1975) 269
[11] Y. D. Bayukov et al., Phys. Rev. **C20**, (1979) 764
[12] S. Frankel et al., Phys. Rev. **C20**, (1979) 2257